Available online at www.sciencedirect.com

ScienceDirect

Procedia Engineering 99 (2015) 33 – 38

Procedia Engineering

www.elsevier.com/locate/procedia

"APISAT2014", 2014 Asia-Pacific International Symposium on Aerospace Technology, APISAT2014

Flutter Influence Mode Analysis of High Speed Wing Model

ZHAO Ling, JI Chen, YANG Yinong, LIU Ziqiang*

China Academy of Aerospace Aerodynamics, 100074, Beijing, P.R.China

Abstract

In flutter wind tunnel test, the matching degree between scaled model and prototype would directly affect the reliability of test results. It is difficult to achieve completely dynamic similarity because of some material or technological constrains, and only lower order modes including mode shape and frequency are accurately simulated to construct a compromised model. Theoretical support would be necessary to answer the question which modes must be simulated to guarantee data validity of wind tunnel flutter test. An analytical study of a sweepback wing has been undertaken to estimate the flutter influence mode needed for accurate flutter prediction by analyzing generalized aerodynamic stiffness coefficient, unsteady aerodynamic force and flutter results. The results show that the aerodynamic stiffness coefficient with expression of mode shape could be taken as a quick criterion for mode selection in flutter model design and analysis.

Peer-review under responsibility of Chinese Society of Aeronautics and Astronautics (CSAA)

Keywords: flutter influence mode; unsteady aerodynamic force; model design

1. Introduction

Flutter Wind tunnel testing is an important approach to assure components of aircraft or a complete vehicle to be free of flutter in their flight envelopes. In the process of test, the matching degree between scaled model and prototype would directly affect the reliability of test results. Flutter model design should follow strictly design specification to satisfy geometric and dynamic similarity. The scaled model is demanded to simulate mode shape of prototype for dynamic similarity requirements [1-4]. Actually it is difficult to achieve completely dynamic similarity because of some material or technological constrains, and only lower order modes can be accurately simulated to

* Corresponding author. Tel.:+86-10-68743224;
*E-mail address:*zhaoling_zlg@163.com

Peer-review under responsibility of Chinese Society of Aeronautics and Astronautics (CSAA)
doi:10.1016/j.proeng.2014.12.504

construct a compromised model. How to choose the modes that needed to be simulated accurately is usually dependent on engineering experiences. Theoretical support should be necessary to select flutter influence modes in flutter model design for guarantying data validity of wind tunnel flutter test.

Actually, judgment of flutter influence mode is also important for linear aeroelastic analysis. Linear aeroelastic stability analysis is based on the assumption that the aerodynamic forces linearly depend on the structural deformation, which is usually expressed in modal coordinates by modal superposition methods. Mode truncation implies that those aerodynamic forces induced by motions of higher mode would be ignored. Modes that have dominant contributions to flutter result must be confirmed and included in flutter analysis. Besides this, flutter influence modes are also required in reduced order model (ROM) for unsteady aerodynamics [5-7]. The ROM constructs models between generalized aerodynamics forces (outputs) and modal coordinates (inputs), whose success is largely depend on the choice of the modal structure and the quality of data.

The principal objective of the studies is carried out to develop an understanding of flutter influence modes and find an effective judging method for flutter influence modes selection. An analytical study of a high speed sweep-back wing has been undertaken to estimate the basic mode orders needed for accurate flutter prediction by analyzing generalized aerodynamic stiffness coefficient, unsteady aerodynamic force and flutter results. By comparing the results, the effects of mode motion to generalized aerodynamic force and flutter characteristic are numerically investigated.

Nomenclature

D	aerodynamic influence coefficient matrix
A	dimensionless stiffness ratio
B	aerodynamic damping matrix
C	aerodynamic stiffness matrix
w	downwash vectors
B^*	generalized damping coefficients
C^*	generalized stiffness coefficients
$\bar{\mathrm{M}}$	generalized structure mass matrix
$\bar{\mathrm{C}}$	generalized structure damping matrix
$\bar{\mathrm{K}}$	generalized structure stiffness matrix
Φ	structural natural mode
q	generalized coordinate
ω	frequency
ρ	density
V	velocity
λ	eigenvalue

2. Methodology

In subsonic and supersonic flow, unsteady aerodynamic forces are usually evaluated using linear aerodynamic panel methods, such as Double-Lattice Method (DLM) and Lifting Surface Method [8-10]. The aerodynamic pressure distribution for each aerodynamic element becomes:

$$\Delta p = \frac{1}{2}\rho V^2 \boldsymbol{D}^{-1} w \tag{1}$$

Where Δp is a pressure vector at pressure control point, D is aerodynamic influence coefficient (AIC) matrix, w represents downwash vectors for aerodynamic elements which is due to the structural oscillation. The downwash vector for aerodynamic element is obtained using the following equation:

$$w = \frac{\partial \phi}{\partial x} q + \frac{\phi}{V} \dot{q} \tag{2}$$

Where V is velocity, q is generalized coordinate and Φ is mode shape vector. Substitution of Eq. (2) into Eq. (1) yields the final generalized unsteady aerodynamic force expression:

$$F = \rho V \boldsymbol{B}\dot{q} + \rho V^2 \boldsymbol{C} q \tag{3}$$

the aerodynamic damping matrix $\boldsymbol{B}$ and aerodynamic stiffness matrix $\boldsymbol{C}$ is:

$$\boldsymbol{B} = \frac{1}{2}\boldsymbol{D}^{-1}\phi^T\phi \qquad \boldsymbol{C} = \frac{1}{2}\boldsymbol{D}^{-1}\phi^T\frac{\partial\phi}{\partial x} \tag{4}$$

from which the generalized damping and stiffness coefficients can be extracted as:

$$\boldsymbol{B}_{ij}^{\ *} = \varphi_i^T\varphi_j \qquad \boldsymbol{C}_{ij}^{\ *} = \left|\varphi_i^T\frac{\partial\varphi_j}{\partial x}\right| \tag{5}$$

The Eq. (3) is coupled with the structural equations to perform aeroelastic analysis:

$$\bar{\boldsymbol{M}}\ddot{q} + (\rho V\boldsymbol{B} + \bar{\boldsymbol{D}})\dot{q} + (\rho V^2\boldsymbol{C} + \bar{\boldsymbol{K}})q = 0 \tag{6}$$

Where $\bar{M}$, $\bar{C}$ and $\bar{K}$ are generalized structure mass, damping and stiffness matrices, respectively. Eq. (6) is formulated in the state-space equation and solved at a set of dynamic pressure values. The root locus method is used to assess the stability of the aeroelastic system. The point at which the root locus crosses the imaginary axis is identified as the flutter dynamic pressure. The eigenvalue λ provide insightful information about the natural frequency ω *and* damp ζ for aeroelastic system.

$$\begin{Bmatrix} \dot{q} \\ \ddot{q} \end{Bmatrix} = \begin{bmatrix} 0 & \boldsymbol{I} \\ -\bar{\boldsymbol{M}}^{-1}(\rho V^2\boldsymbol{C} + \bar{\boldsymbol{K}}) & -\bar{\boldsymbol{M}}^{-1}(\rho V\boldsymbol{B} + \bar{\boldsymbol{D}}) \end{bmatrix} \begin{Bmatrix} q \\ \dot{q} \end{Bmatrix} \tag{7}$$

$$\lambda_i = -\zeta_i\omega_i + j\omega_i\sqrt{1-\zeta_i^2} \tag{8}$$

3. Numerical Test Case

A high speed wing model is analyzed as a numerical example. The example wing model has a span of 0.5 m, an average chord of 0.85 m, a panel taper ratio of 0.4167, and a 60 deg leading edge sweepback angle. Its structural model and dimensions are shown in Figure 1(a). The model's first 10 natural frequencies are given in Table 1, and the node lines of first two modes are shown in Figure 1(b). It can be seen that the first elastic mode is primarily the first bending mode, and the second one is the first torsion mode.

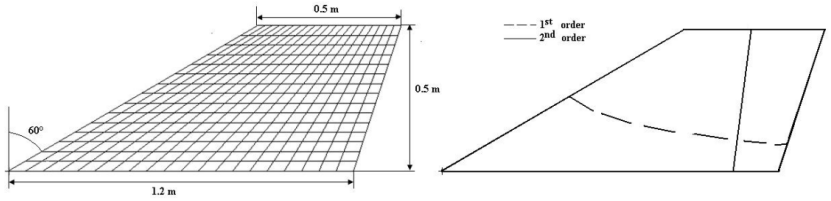

Fig1. (a) schematics of wing geometry and structural model; (b) structural mode shape of the wing

Table 1.Natural frequency of the wing

Mode.	1	2	3	4	5	6	7	8	9	10
Freq.(Hz)	34.53	74.60	151.21	208.22	251.17	313.20	373.65	486.55	513.30	577.17

A corresponding flutter result at sea level is predicted by second-piston theory aerodynamics [11-13] and assuming zero structural damping. The state-space approach predicts a flutter speed of 1951.2m/s and flutter frequency of 72.7Hz.The results of eigenvalue are plotted in Fig 2. Results of aerodynamic damping versus velocity presented in Figure 2 (a) show that: the first mode (bending mode) turns downward toward a very stable condition just as the second mode (torsion mode) heads for instability, leading to flutter. The imaginary part of the eigenvalue corresponding to frequency is plotted versus velocity in Fig 2 (b). In this plot two frequencies are seen to coalesce as the instability approached, which depicts that the flutter mechanism is primarily the coupling between the first and second elastic modes.

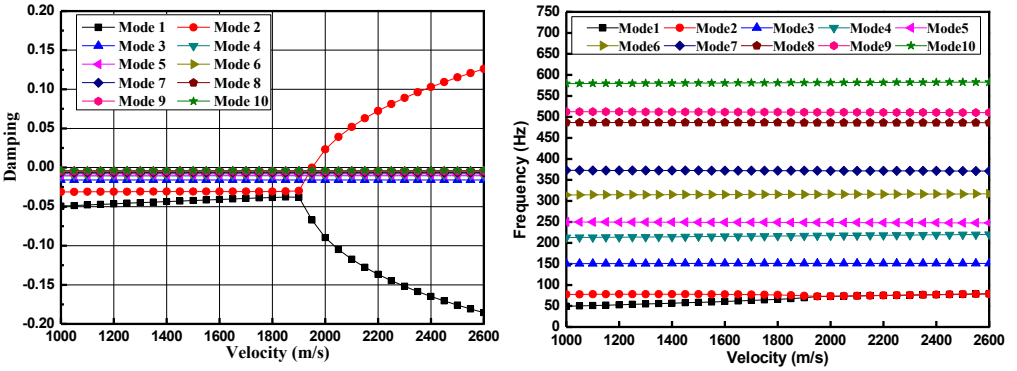

Fig2. Flutter results for wing model (a) v-g plots; (b) v-f plots

The contribution coefficients of the first ten elastic modes to flutter mode is given in Table 2. The coefficient for first mode is 85.45%, and 100% for second mode. The results of v-f plot and contribution data present that the first and second modes are flutter primary modes which must be simulated exactly in designing of flutter models and adopt in aeroelastic analysis. The other modes which also have dominant contributions to flutter results should be further confirmed.

Table 2.Contribution of elastic modes to flutter mode

Mode.	1	2	3	4	5	6	7	8	9	10
Present.(%)	85.45	100.00	9.79	2.44	0.05	0.83	0.06	0.02	0.004	0.01

3.1. Generalized Aerodynamic Stiffness Coefficients

For bending–torsion flutter, the damping contribution is unimportant. Structural damping could be neglected and quasi-steady or quasi-static aerodynamic model is feasible for flutter solutions [14]. The phenomenon of flutter can be explained by the frequency coincidence theory directly, which presents the important role of aerodynamic stiffness. Study would be next carried out in the framework of aerodynamic stiffness to estimate flutter primary modes and influence modes.

(1) Flutter Mode Estimation

The stiffness ratio of aerodynamic and structural reflects the influence degree of aerodynamic force to structural motion. The greater value means the more energy got by structure from airflow and great change infrequency.

In order to facilitate the aeroelastic applications, a dimensionless stiffness ratio parameter is defined:

$$A_i = C_{ii}^* / (\frac{\omega_i}{\omega_1})^2 \tag{9}$$

Where C_{ii}* is the main stiffness coefficients of i^{th} vibration mode, representing relative magnitude of aerodynamic stiffness, ω_i is frequency of i^{th} mode, representing relative magnitude of structural stiffness. We can estimate the flutter primary mode by comparing A_i value of each mode.

Figure 3 presents the stiffness ratio value of first 10 modes in histogram plot. One observes large amplitude in first, second and forth mode which implies evident change in frequency with the increase of airspeed. The results are consistent with trends in V-f plot. It can be deduced that the 1st, 2nd and 4th mode are likely to be flutter primary mode under different flow condition.

(2) Flutter Influence Mode Estimation

A parameter C_{ij}* (Eq.5) is introduced to analyze the effect of mode motion to generalized aerodynamic force. C_{ij}* is the generalized aerodynamic stiffness coefficient in i^{th} mode due to unit-amplitude harmonic motion of the j^{th} mode. Once the mode-dependent C_{ij}* are calculated, these aerodynamic force brought by mode variation can be evaluated.

Shown in Figure4 is a comparison of the aerodynamic stiffness coefficient C_{ij}*for first and second elastic mode due to motion of first ten modes. As can be seen from the figure, for first mode (first bending mode), the maximum value is ascribed to motion of itself, and the next are from motions of 2nd,3rd and 4th mode, whose relative proportions are 29%,9% and 14%, respectively, compared to the main coefficient C_{11}*. For second mode (first torsion mode), the maximum value C_{2j}* is due to motion of 1st mode. And the 2nd, 3rd and 4th modes also have effects on its aerodynamic stiffness. The results show that the first four modes are important to the aerodynamic stiffness coefficients of flutter primary modes.

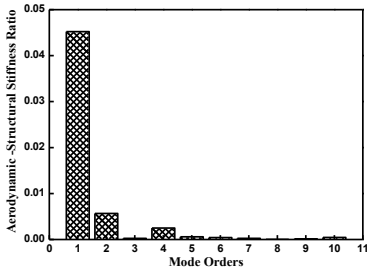

Fig3.Aerodynamic-Structural Ratios

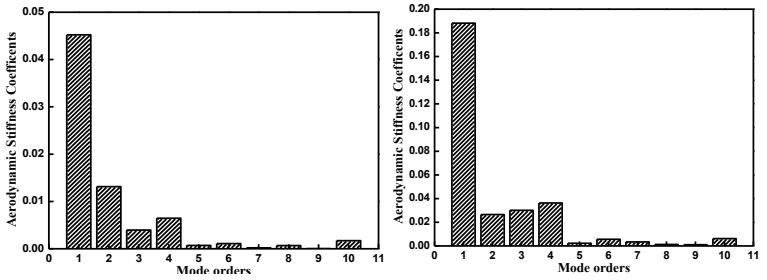

Fig4.Generalized Aerodynamic Stiffness Coefficient(a)1st mode; (b) 2nd mode

3.2. Generalized Aerodynamic Force Analysis

Giving that the wing model is oscillating in form of harmonic motion of each mode: $q=a\cdot\sin(\omega t+\theta)$, where a is the mode amplitude, ω is oscillating frequency. Considering the mass-normalized mode shapes are used in analysis, the kinetic energy would keep invariability for same mode amplitude and oscillating frequency. The aerodynamic pressure distributions due to the motion of each mode are predicted by second-piston theory aerodynamics, and integrated over the wing model surface to yield the generalized aerodynamic force of first and second modes.

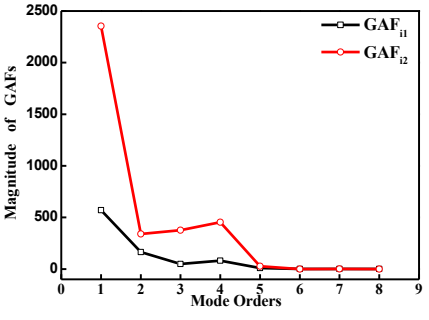

Fig5. Magnitudes of GAFs of 1st and 2nd modes

Fig 6. Variation of Flutter Speed with Mode Number

The results at condition of A=0.01 and V=1500m/s are illustrated in Figure 5. As can be seen from the figure, in general GAFs of 2nd mode (first torsion mode) are larger than 1st mode (first bending mode). The GAFs of 2nd mode

obtained from 1st mode motion is biggest whose magnitude is 10^3, and the GAFs obtained from 2nd, 3rd and 4th mode motion has magnitude of 10^2, the GAFs induced by high order modes has magnitude of 10^1. The first four modes can provide more exactly aerodynamic force to flutter primary modes.

3.3. Flutter results analysis

Mode truncation method is employed to obtain flutter velocity of wing model, and effects of cutting mode numbers on flutter result are evaluated. Figure 6 presents the variations of the flutter speed due to the variation of the mode truncation orders. The result continue to rise around 2~4 modes, after the jump there is a smooth decrease in flutter speed. Although the error is less than 10% in flutter velocity when using first two modes, it will exceed 17% in dynamic pressure. When first four modes are used, the error in dynamic pressure will be less than 3%. Comparison of the flutter results using different mode orders shows that using flutter primary modes only f can cause error, addition of flutter influence mode may improve the result.

4. Conclusion

The paper has presented an effective methodology for flutter influence modes judgment. A set of parameters is used to address flutter influence modes, including generalized aerodynamic stiffness coefficient, unsteady aerodynamic force and flutter results. Through numerical comparison of the sweepback wing model, the choice of flutter influence modes is revealed. The results show that the aerodynamic stiffness coefficient with expression of mode shape could be taken as a quick criterion for flutter influence mode selection in flutter model design and analysis.

References

[1] Guan D, Aircraft aeroelasticity handbook, first ed., Beijing: Aviation Industry Press;1994:215-217.
[2] John K. Ramsey, NASA aeroelasticity handbook, Volume 2: Design Guides, NASA/TP-2006-212490-VOL2-PART2, Cleveland: NASA Glenn Research Center, November 2006.
[3]M. Baker, P. Lenkey, Parametric flutter analysis of the TCA configuration and recommendation for FFM design and scaling, CRAD-9408-TR-3342, Seattle, WA: The Boeing Company, November 21, 1997.
[4] Edwards John W., Schuster David M., Spain Charles V., et al. MAVRIC flutter model transonic limit cycle oscillation test, AIAA paper 2001-1291, Seattle, WA: AIAA/ASME/ASCE/AHS/ASC structures, structural dynamics and materials conference, April 16-19, 2001.
[5] Raveh, D.E, Identification of CFD-based unsteady aerodynamic models for aeroelastic analysis, 44th AIAA/ASME/ASCE/AHS Structures, Structural Dynamics, and Materials Conference. Norfolk, VA. 2003.
[6]Prazenica R.J., Lind R. and Kuidila A.J, Uncertainty estimation from Volterra kernels for robust flutter analysis, 43rd AIAA/ASME/ASCE/AHS/ASC Structures, Structural Dynamics, and Materials Conference. Denver, Colorado. 2002.
[7]D. D. Liu, P. C. Chen, Flutter analysis with structural uncertainty by using CFD-based aerodynamic ROM, NATO-AVT-154.
[8] Chen G B, Zou C Q, Yang C, Aeroelastic design foundation,Beijing: Beijing University of Aeronautics and Astronautics Press,2004:81-82.
[9] J.P. Giesing, T.P. Kalman, W.P. Rodden, Subsonic unsteady aerodynamics for general configurations, AIAA paper No. 72-26, San Diego, California: AIAA 10th Aerospace Sciences Meeting, 1972.
[10] ATLEE M. Cunningham, JR, The Application of general aerodynamic lifting surface elements to problems in unsteady transonic flow, NASA CR-112264, 1973.
[11] Milton D. Van Dyke, A study of second-order supersonic-flow theory, NACA TN 2200, Washington: California Institute of Technology, January 1951.
[12] Jack J. McNamara, Andrew R. Crowell, Approximate modeling of unsteady aerodynamics for hypersonic aeroelasticity, Journal of Aircraft, Vol.47,No.6,2010: 1932-1945.
[13] Yang Binyuan, Song Weili, Expressions about aerodynamic forces of flutter for wing with high angle of attack by local flow piston theory, Journal of Shanghai Mechanics, 1999,20(3).
[14] E.H. Dowell, Aeroelasticity modern Tutorial , Chen Wenjun, Yin Chuanjia, translated. Beijing: Astronautic Publishing House, 1991: 67-69.